Journal of Sound and Vibration (1999) **219**(3), 451–481
Article No. jsvi.1998.1846, available online at http://www.idealibrary.com.on IDEAL

ELECTROPNEUMATIC TRANSDUCERS AS SECONDARY ACTUATORS FOR ACTIVE NOISE CONTROL PART III: EXPERIMENTAL CONTROL IN DUCTS WITH THE SUBSONIC SOURCE

L. A. BLONDEL†

Faculté Polytechnique de Mons, Laboratory of Acoustics, 9 rue de Houdain, B-7000 Mons, Belgium

AND

S. J. ELLIOTT

Institute of Sound and Vibration Research, The University of Southampton, Southampton SO17 1BJ, England

(*Received* 17 *March* 1998, *and in final form* 9 *July* 1998)

The possibility of performing active control of periodic noise propagating in ducts using a subsonic electropneumatic acoustic generator as secondary source is investigated. The subsonic generator has been studied both theoretically and experimentally in two companion papers, and this sound source was shown to be highly efficient, but non-linear. The non-linear behaviour of the source decreases as the acoustic pressure at its output is reduced, however, as in the case when the source is used as a secondary actuator in an efficient active control system and thus the source is well suited to such applications. Residual non-linearities of the subsonic source are shown to be due to the mechanical design of the actuator. An harmonic controller is discussed which accounts for the residual non-linear behaviour of the subsonic source. Experiments carried out with a manual version of this controller, that controls the first five harmonic components of the signal driving the subsonic source, reveal that it is efficient in controlling periodic primary sound fields. The implementation of a fully coupled harmonic controller is, however, shown to require large processing capacities. A theoretical analysis of a simplified version of the harmonic controller—the decentralized harmonic controller—is carried out, and simple conditions are established under which the decentralized controller offers similar performances to the fully coupled harmonic controller. These conditions are shown to be satisfied when using the subsonic source as a secondary actuator. The non-linear behaviour of the subsonic source can also cause a further problem, since the error surface experienced by the control system may exhibit local minima. It was found that the likelihood of this happening was much reduced is only the fundamental component of the harmonic controller was adapted initially, and then the other harmonics were changed in a second phase of adaptation. The implementation of a decentralized harmonic controller is considered, using a dual channel signal processing board. A purely

†Present address: Alston, Signalling Group, B.P. 4211, B-6001 Charleroi, Belgium.

0022–460X/99/030451 + 31 $30.00/0

linear model for the plant under control is shown to be accurate enough for modelling the system under control and to ensure convergence of the controller. Experiments with the automatic controller reveal that attenuations measured at the monitor microphone are around 25 dB, for sinusoidal primary sound fields.

1. INTRODUCTION

Electropneumatic acoustic generators operate by the release of compressed air through an aperture, the area of which is made to vary with time. Both theoretical and an experimental analysis of these generators were presented in two companion papers [1, 2], in which it was demonstrated that a subsonic source, in which the Mach number in the throat is significantly less than one, can be highly efficient but is potentially non-linear in its operation. The operating equation of subsonic electropneumatic sources was shown to be

$$Q_2(t) = A_1(t)\sqrt{C_d(p_{pl} - p_2(t))/\rho} \tag{1}$$

in which $Q_2(t)$ is the volume flow into the duct to which the source is connected, C_d is the discharge coefficient of the orifice modulating the airflow, p_{pl} is the steady plenum pressure, $p_2(t)$ is the time varying pressure at its output, and ρ is the density of the fluid. The non-linearity in operation arises from the dependence of the volume velocity, $Q_2(t)$, on the pressure at the output of the source, $p_2(t)$, as well as on the area of the opening, $A_1(t)$. If, however, the source were used in an active control system in which $p_2(t)$ was cancelled, the source would become linear again, and it is this observation which prompted the work reported here. Despite its non-linear behaviour, the high efficiency and the robustness of the subsonic source make it a good candidate for use as a secondary actuator in active noise control, and the main objective of this paper is to investigate this possibility both theoretically and experimentally. This paper is organized as follows. Section 2 describes the active control problem considered and briefly reviews the literature on active control in non-linear systems. Section 3 reports an experimental investigation of the behaviour of the subsonic source when performing active control and discuss the choice of a reliable controller. Sections 4 and 5 describe the investigation of this controller, from a theoretical and an experimental point of view. Section 6 is devoted to an experimental analysis of the error surface, whose shape has a significant influence on the behaviour of the controller. Finally, section 7 presents the results of active noise control experiments achieved with an automatic controller implemented on a signal processing board.

2. ACTIVE CONTROL IN DUCTS

An important potential application of active control is the control of sound in ducts. In many industrial applications the duct is carrying hot, potentially corrosive gas and the sound pressure levels are high. There is thus a requirement for a robust secondary actuator capable of generating large volume velocities. In the specific example of automobile exhaust noise the main advantage of active control over passive methods is that it reduces both the pressure drop through the

exhaust pipe and the weight and size associated with the silencing systems, leading to a reduction in the vehicle consumption. The fundamental difficulty in applying active control in this application lies in transducers, and more particularly in secondary sources: the diaphragm of an electrodynamic loudspeaker placed in the exhaust pipe is likely to be quickly damaged by the high temperature (about 300°C in normal conditions) exhaust gas flow. This difficulty was recognized by Roure [3], who noted the difficulty of designing loudspeakers able to resist extreme environments. Electropneumatic acoustic generators appear to be particularly applicable in this case since the design of these generators makes them able to resist hot, humid and corrosive environments. Subsonic sources seem particularly interesting in this application since they offer a high pneumatic efficiency. The possibility was thus investigated of adapting the subsonic source for the control of acoustic plane waves travelling in ducts (see Figure 1). The control of plane waves in ducts is a classical problem in active control, that has received a lot of attention in the last two decades. It is a well documented area, and commercial systems for the control of broadband noise in air conditioning ducts have been available for some years. An exhaustive list of the patented literature on the subject was presented by Guicking [4]. The acoustical objective is generally to create a pressure null in the vicinity of a monitor microphone, in general placed close to the secondary source output, so that the incident sound is reflected by the impedance discontinuity. For problems in which the unwanted disturbance can be detected prior to its arrival at the position in space where control is required, this acoustical objective is generally achieved by using feedforward control. For noise propagating in the exhaust pipe of an internal combustion engine, one can observe that (i) the waveform is almost periodic, at least over short periods of time, (ii) a convenient, non acoustic reference signal is available, from the ignition circuit of the engine for example—acoustic feedback between the secondary source and the reference sensor is not likely to occur and so the control is purely feedforward in nature, which simplifies the control algorithm, (iii) the noise in the exhaust pipe is dominated by a tonal component at the engine firing frequency, that is likely to range between about 20 and 200 Hz, depending on the engine rotational speed.

In summary, the problem is to control adaptively a tonal noise by using a purely feedforward approach, the acoustical aim being the creation of a pressure null in the vicinity of the error microphone. The structure of the controller as well as the control algorithm will depend on whether the physical system under control has a linear or non-linear nature. A linear active control system is a system in which

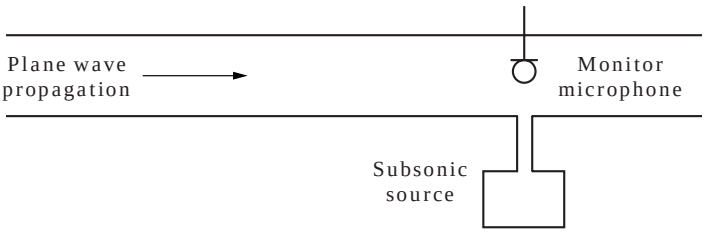

Figure 1. Active control of noise travelling in ducts. The duct cross-section is assumed to be small enough to guarantee plane-wave propagation.

both the sound propagation and the behaviour of the secondary source can be considered as reasonably linear. In most cases, the controller is implemented by using an adaptive FIR filter, whose cofficients are in general updated by using the filtered-X algorithm, as introduced for active control by Burgess [5]. The aim of the procedure is to adjust the filter coefficients in such a way that the mean squared error is minimized. An exhaustive discussion of the algorithm and of its features has been given, for example, by Nelson and Elliott [6]. Secondary sources used for active noise control are often assumed to behave linearly. Strictly speaking this assumption is not often fulfilled, even when using electrodynamic loudspeakers as secondary actuators. Non-linearities in these actuators were discussed for example by Birt [7], Klippel [8], and more recently by Beltran [9]. The non-linear behaviour of electrodynamic loudspeakers is likely to increase when they are required to generate high amplitude low frequency acoustic pressures. In most practical cases however, non-linearities in well designed electrodynamic loudspeakers are weak enough so that these systems can be considered as reasonably linear. The situation can be rather different when considering the active control of structural vibrations, where the actuator applying the secondary vibration can sometimes exhibit a strongly non-linear behaviour. A good example is the magnetostrictive actuator, that is subject to a significant magnetic hysteresis [10]. The secondary actuator is not the only potential source of non-linearities in active control applications: the response of the system under control may also be non-linear. This may, for example, occur when controlling vibrations in structures, since, in particular, the coupling between different parts of the structure can be non-linear, or when controlling very high amplitude sound waves propagating in air or in other media [11]. Non-linear control systems hence refer to systems in which the plant and/or the secondary actuator(s) behave non-linearly. The use of an adaptive non-linear filter as the controller may be a way to increase the performance of the active control system under these non-linear conditions. Klippel [11] suggested the use of a controller based on a Volterra filter. A non-linear controller can also be implemented on the basis of an artificial neural network. This possibility seems to have mainly been considered from a theoretical point of view [12], and although some simulations revealed encouraging results, no experimental work seems to have been carried out so far. The main reasons are probably that the implementation of a neural network often require a large processing capacity and that the convergence of the network is sometimes likely to cause problems [11]. The behaviour of neural networks is also far from being fully theoretically understood. Sutton and Elliott [13, 14] suggested performing feedforward control in non-linear systems using an harmonic controller. The principle of the harmonic controller is to synthesize a signal that, when filtered by the non-linear system under control, produces a signal that is as close as possible to the inverse of the primary periodic disturbance. To achieve this objective, a sinusoidal reference signal, at the same fundamental frequency as the disturbance, is applied to a non-linear device so that a set of in-phase and quadratic harmonics is generated. The controller then forms a linear combination of the weighted harmonics, and the resulting signal drives the non-linear system. The procedure implicitly depends on the assumption that the non-linear system generates an output at the same

fundamental frequency as its input, with no subharmonics. It is important to note that the harmonic controller is, by nature, only able to perform the control of *periodic* primary disturbances.

3. ACTIVE CONTROL WITH THE SUBSONIC SOURCE

The literature review of the previous section suggests that a good knowledge of the nature of the system under control is necessary for designing an efficient controller. Non-linearities in the subsonic electropneumatic generator were discussed in reference [1], and the main source of non-linearity was shown to be the time-varying acoustical resistance of the throat, which depends on the flow through it. The fundamental equation of subsonic sources [equation (1)] explicitly shows that the larger the variations of the acoustic pressure $p_2(t)$ at the source output compared to the plenum pressure p_{pl}, the more non-linear the source. This conclusion is illustrated by the results shown in Figure 2, which show the harmonic contents in the acoustic pressure at the subsonic source output when connected to two acoustic loads, one of which has a higher acoustic impedance and thus generates a higher output pressure.

When the subsonic source is acting as secondary source in an efficient duct active control system, the acoustic pressure at its output should become negligible. The source should in this case behave linearly, at least in the steady state, after the transient adaptation phase is over. The validity of this important assumption was checked experimentally, by using a manual control procedure similar to that suggested by Conover [15]. The experimental procedure can be summarized as

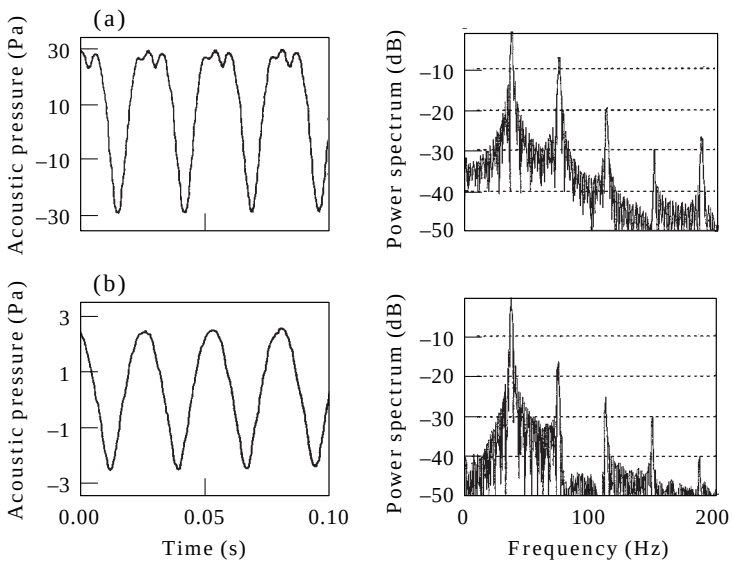

Figure 2. Acoustic pressure measured at the output of the subsonic source. Experimental conditions: $f = 37$ Hz, plenum pressure is 60 Pa above the atmosphere pressure. (a) Acoustic pressure at the source output when connected to an acoustic impedance whose resistive part is about equal to 10^6 N s/m^5; (b) acoustic pressure at the source output when connected to an acoustic impedance whose resistive part is about equal to 10^4 N s/m^5.

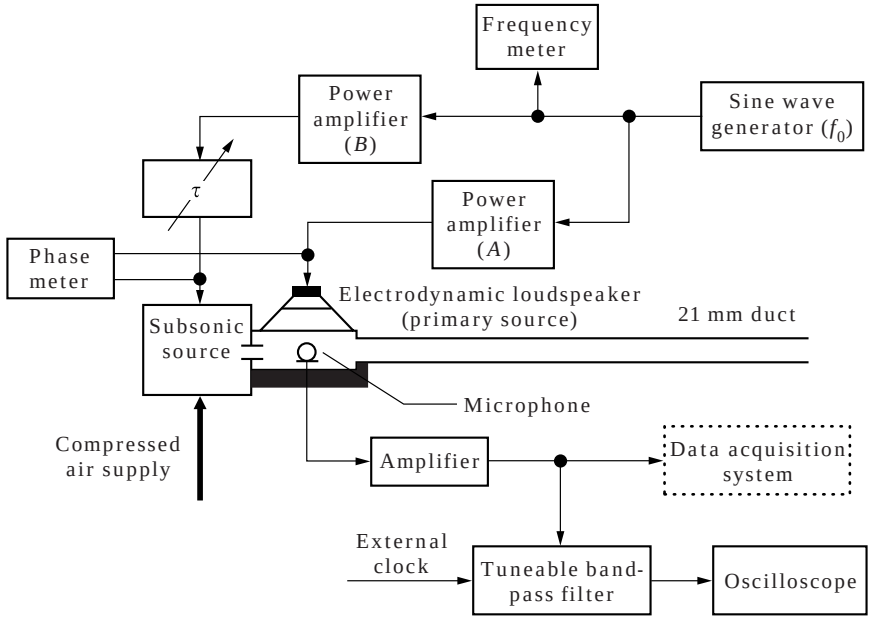

Figure 3. Experimental set-up for manual active noise control experiments with the subsonic electropneumatic source. The fundamental component at the monitor mcirophone was the only one to be controlled.

follows, with reference to Figure 3. The laboratory subsonic source described in reference [2] acted as the secondary source and was connected to a 3·4 m long, 21 mm diameter circular duct, and an electrodynamic loudspeaker, placed near the output of the electropneumatic actuator and driven with a sinusoidal voltage at frequency f_0, acted as the primary source. The loudspeaker and the subsonic source was acting as the secondary source. The aim of the control procedure was to minimize the acoustic pressure at the location of a monitor microphone placed about 25 cm away from the subsonic source output. The electrodynamic shaker driving the subsonic source was fed with a sinusoidal current also at frequency f_0 and the throat area was fully modulated. The pneumatic source was adjusted in phase prior to control, to ensure that both the primary and secondary sources were generating approximately equal volume velocities. This adjustment was performed by controlling the plenum pressure of the subsonic source. The minimization of the acoustic pressure at the microphone location was then carried out by manually adjusting the delay τ between the secondary and primary waveforms, as shown in Figure 3, which modified the phase shift between the contributions at the monitor microphone of acoustical signals driven by both the primary and the secondary source. The procedure of manual control ended when the fundamental component of the signal at the monitor microphone was reduced to a minimum value. This fundamental component was viewed on an oscilloscope, after being filtered by using a band-pass filter tuned on the frequency f_0. The phase shift $\Delta\phi$ between sinusoidal signals feeding the subsonic source and the loudspeaker was measured by using a phasemeter. The (non-filtered) signal picked up by the microphone was also recorded at various stages during the manual control procedure. Experiments

were carried out at various frequencies and for various levels of the signal driving the electrodynamic loudspeaker. The results achieved are summarized in Figure 4, for four frequencies f_0: 35, 45, 60, 100 Hz. For each set of experimental conditions, the figure illustrates the acoustic pressure at the microphone location when the subsonic source is acting alone at various stages during the active control procedure of the magnitude of the fundamental component at the monitor microphone. The harmonic content of the acoustic pressure at the source output is shown to decrease as the active control procedure reduces the amplitude of the fundamental component of this acoustic pressure, which was expected from the above discussion. This harmonic contents is, however, not totally, cancelled out

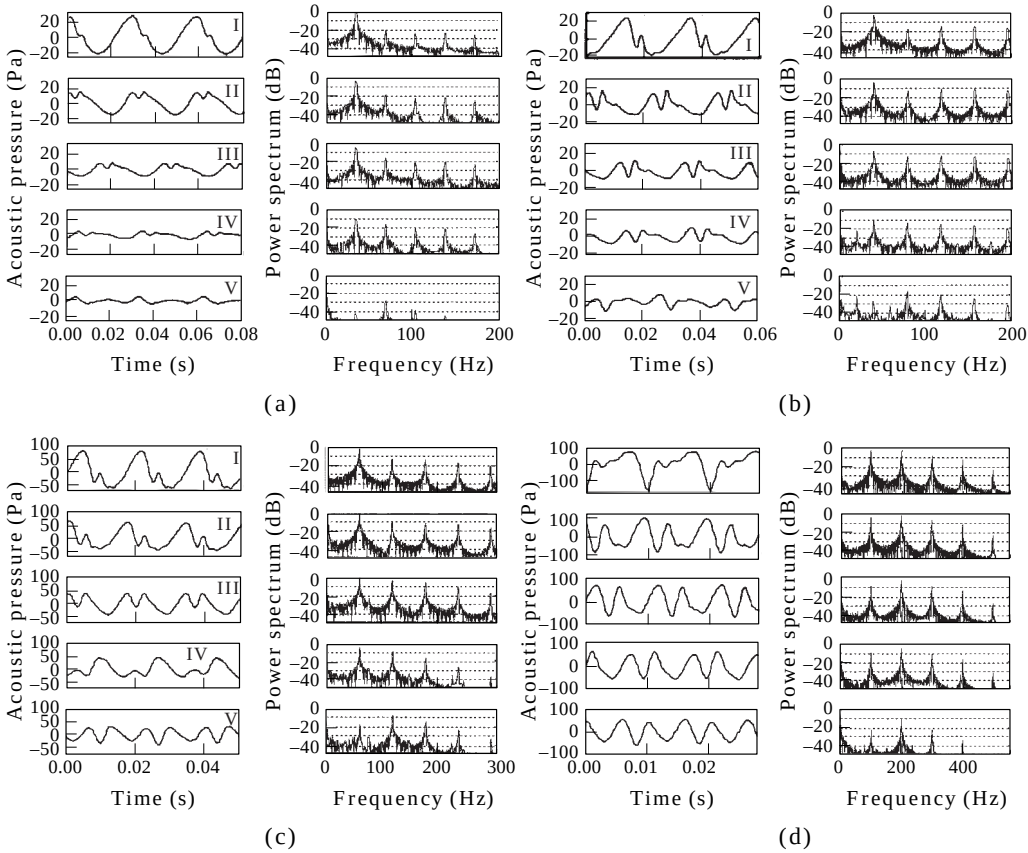

Figure 4. Acoustic pressure waveform and spectra at the microphone location, at various stages during the manual active control procedure and at four different frequencies. (a) $f_0 = 35$ Hz, $p_{pl} = p_{atm} + 53$ Pa, (I) subsonic source is acting alone; (II) active control, $\Delta\phi = 170°$; (III) active control, $\Delta\phi = 180°$; (IV) active control, $\Delta\phi = 190°$; (V) active control, $\Delta\phi = 198°$. (b) $f_0 = 45$ Hz, $p_{pl} = p_{atm} + 68$ Pa, (I) subsonic source is acting alone; (II) active control, $\Delta\phi = 165°$; (III) active control, $\Delta\phi = 175°$; (IV) active control, $\Delta\phi = 185°$; (V) active control, $\Delta\phi = 194°$. (c) $f_0 = 60$ Hz, $p_{pl} = p_{atm} + 134$ Pa, (I) subsonic source is acting alone; (II) active control, $\Delta\phi = 185°$; (III) active control, $\Delta\phi = 195°$; (IV) active control, $\Delta\phi = 205°$; (V) active control, $\Delta\phi = 212°$. (d) $f_0 = 100$ Hz, $p_{pl} = p_{atm} + 274$ Pa, (I) subsonic source is acting alone; (II) active control, $\Delta\phi = 150°$; (III) active control, $\Delta\phi = 160°$; (IV) active control, $\Delta\phi = 170°$; (V) active control, $\Delta\phi = 177°$.

when the amplitude of the fundamental becomes negligible. The residual non-linear behaviour of the subsonic source may be ude to the following effects.

(i) The friction between the slider and its housing introduces a non-linearity in the slider movement, as explained in reference [2]. In other words, driving the electrodynamic shaker of the subsonic source with a sinusoidal signal does not guarantee the throat area versus time $A_1(t)$ to be strictly sinusoidal.

(ii) There is a non-negligible alternating component in the plenum pressure due to acoustical resonances in the plenum chamber, as also explained in reference [2], and second and third harmonic components appear in the power spectrum of this alternating component.

(iii) The discharge coefficient C_d at the throat may not be completely constant along the cycle of operations of the source.

(iv) The fundamental component of the signal at the monitoring microphone was not totally cancelled out.

(v) The eletrodynamic loudspeaker acting as primary source behaved slightly non-linearly.

(vi) The monitoring microphone was placed about 25 cm away from the output of the subsonic source. The acoustic pressure was therefore reduced 25 cm away from the subsonic source output, and not exactly at the output of this source.

The residual non-linear behaviour of the subsonic source limits the attenuations at the error microphone, that were measured to be between 18 and 25 dB for sinusoidal primary acoustic fields. Three potential ways of reducing the magnitude of these residual harmonics can be identified. The first possibility would be to use a linear controller driven by a filtered-X LMS algorithm, whose aim would be to minimize only the amplitude of the fundamental frequency component of the acoustic pressure at the source output, while mechanically redesigning the subsonic source to increase the linearity of the slider movement and to decrease the magnitude of the alternating part in the plenum pressure. The advantages of this solution are that the filtered-X LMS algorithm is well documented and easy to implement. However, this solution has two major drawbacks. First of all, proper working of the filtered-X LMS algorithm requires an estimate of the transfer function of the electroacoustic error path between the secondary source input and the error microphone output. The characteristics of the error path can be expected to vary during the control procedure, since the behaviour of the subsonic source directly depends on the acoustic pressure at its output and this variation of the error path could affect the convergence of the filtered-X LMS algorithm during the transient phase of the control procedure. It was, however, shown by Morgan [16] and, more recently, by Elliott *et al*. [17] that the filtered-X LMS algorithm is very robust to errors in the estimation of the true error path. For a single channel system with a pure tone reference signal (frequency f_0), the phase of the estimated path at f_0 must be within only $\pm 90^\circ$ of that of the true path to ensure convergence. This important result shows that the estimate of the error path need not be very accurate. The second drawback of this solution is that reworking the mechanical

design of the subsonic source would be a costly and time consuming operation. Its success is even not guaranteed since the reduction of the plenum pressure variations was proven in reference [2] to be difficult in practice. A further problem is that depending on the magnitude of the modulation of the throat area, the discharge coefficient is likely to vary along the cycle of operation of the source. Reducing this non-linearity in practice would require a complete remanufacture of the valve of the system.

The second possibility for increasing the measured attenuation at the error microphone would again be to use a linear controller driven by a filtered-X LMS algorithm, while linearizing the subsonic source, by using a predistortion processor of the form described in references [1] and [2]. The procedure for the active control application is, however, rather different from that when the actuator is used as a normal acoustic source. First of all, linearization must be performed when the active control system has reached a steady state of operation, since the degree of non-linearity of the subsonic source depends directly on the acoustic pressure at its output. Secondly, the computation of the signal of predistortion can no longer be based on the analytic equation (1) describing the acoustical behaviour of the subsonic source, because the interaction with the primary sound field must now be taken into account. In comparison to the linearization procedure of the subsonic source when used as a stand alone generator [1, 2], the complexity of the linearization procedure in the current case can therefore be expected to increase. The advantages of this solution are similar to that described above: i.e., the filtered-X LMS algorithm is well documented and easy to implement. This last advantage is counterbalanced by the necessity of implementing quite a complex procedure of linearization, which may require large processing capacities. Because of the frequency response of the electrodynamic shaker driving the subsonic source, some difficulties can also be expected for locally linearizing this actuator at frequencies larger than 50 Hz, as demonstrated in reference [2].

The third possibility for increasing the performance of the active control system would be to use a non-linear controller. The brief literature review of section 2 suggested that the choice of a suitable controller for reducing the primary disturbances in a non-linear system was not straightforward, and depended strongly on the nature of the non-linear system under control. Each of the three methods described (Volterra filter, neural network, harmonic controller) has advantages and drawbacks, and potentially involves high computational burdens. In the current application, the harmonic controller, because of its structure, appears to be a good candidate for controlling periodic primary acoustic disturbances with the secondary subsonic source. To investigate the potential of the harmonic controller in reducing the residual non-linear behaviour of the subsonic source when performing active control, preliminary experiments were performed using a manual version of the harmonic controller. The experimental set-up used to perform these experiments is illustrated on Figure 5. A manual harmonic controller was implemented using a dual channel signal processing board. One channel was used to generate a sinusoidal output at f_0, which was used to drive the electrodynamic loudspeaker acting as the primary source. The other

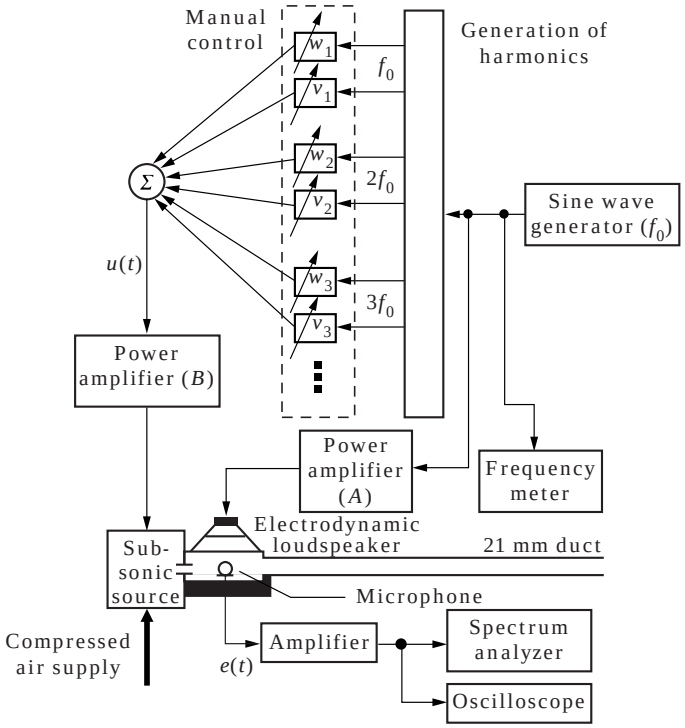

Figure 5. Experimental set-up for manual active noise control of a tonal primary disturbance with an harmonic controller. In practice, the generation of the signal driving the primary source and the generation of signal $u(t)$ were performed by using a dual channel signal processing board.

channel was used to drive the subsonic source. This output $u(t)$ was synthesized according to the equation

$$u(t) = [w_1 \cos(\omega_0 t) + v_1 \sin(\omega_0 t)] + [w_2 \cos(2\omega_0 t) + v_2 \sin(2\omega_0 t)] + \cdots + [w_5 \cos(5\omega_0 t) + v_5 \sin(5\omega_0 t)], \quad (2)$$

in which $\omega_0 = 2\pi/f_0$ and in which the amplitudes w_k and v_k of the in-phase and quadrature components of the fundamental and of the first four harmonic components were adjusted manually, the aim being again to minimize the acoustic pressure in the vicinity of a monitoring microphone located 25 cm away from the subsonic source output. In order to evaluate the efficiency of the control procedure, the output from the monitoring microphone was analyzed by using an oscilloscope and a spectrum analyzer. The manual control of tonal noise using the harmonic controller was performed for the same four fundamental frequencies as above, i.e., 35, 45, 60, 100 Hz. The experimental results are presented in Figure 6. For each frequency, both the acoustic pressure at the microphone location when the subsonic source is acting alone and the acoustic pressure at the microphone location when optimal harmonic active control is achieved are presented. Figure 7 shows the harmonic contents of the error signal at the monitor microphone when the subsonic source is acting alone, when only the fundamental of the error signal is manually controlled and when the fundamental and the first four harmonics of this signal are manually controlled. Manual control of the fundamental and of the

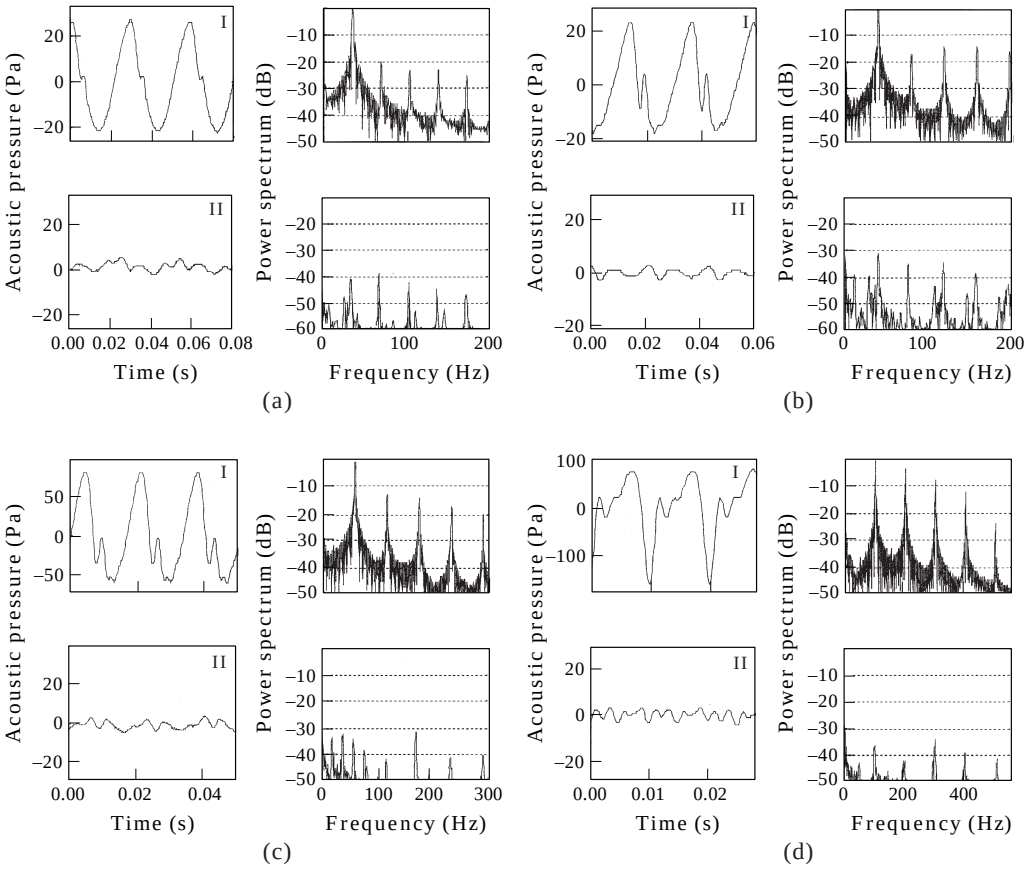

Figure 6. Acoustic pressure versus time and frequency at the microphone location, (I) when the subsonic source is acting alone and (II) for optimal manual harmonic control of the fundamental and of the first four harmonic components. (a) $f_0 = 35$ Hz, $p_{pl} = p_{atm} + 53$ Pa; (b) $f_0 = 45$ Hz, $p_{pl} = p_{atm} + 68$ Pa; (c) $f_0 = 60$ Hz, $p_{pl} = p_{atm} + 134$ Pa; (d) $f_0 = 100$ Hz, $p_{pl} = p_{atm} + 274$ Pa.

first four harmonics leads to reductions larger than 17 dB for all these harmonics, the attenuations measured at the monitoring microphone were this time between 25 and 31 dB. It is clear that a significantly lower mean square error can be achieved by using a harmonic controller rather than one at which only the fundamental frequency is controlled. The implementation of an automatic version of the hrmonic controller is now considered.

4. THEORETICAL ANALYSIS OF THE HARMONIC CONTROLLER

The task of the automatic controller is to adaptively adjust the weights $\mathbf{w} = [w_1, w_2, \ldots, w_n]$ of the N in-phase components and $\mathbf{v} = [v_1, v_2, \ldots, v_n]$ of the N quadrature components so that a cost function J defined as follows is minimized:

$$J = \frac{1}{T_p} \int_0^{T_p} e^2(t)\, \mathrm{d}t. \tag{3}$$

Here T_p is the period of the primary disturbance and the error signal $e(t)$ is defined in Figure 5. Upon assuming that the error signal $e(t)$ can be approximated by a finite summation of N harmonics,

$$e(t) \cong \sum_{n=0}^{N} [a_n \cos(n\omega_0 t) + b_n \sin(n\omega_0 t)], \tag{4}$$

the cost function can be expressed in terms of the Fourier components of the error, by Parseval's theorem, as

$$J \cong \tfrac{1}{2}(\mathbf{a}^{\mathrm{T}}\mathbf{a} + \mathbf{b}^{\mathrm{T}}\mathbf{b}) \tag{5}$$

in which vectors $\mathbf{a} = [a_0, a_1, \ldots, a_n]$ and $\mathbf{b} = [b_0, b_1, \ldots, b_n]$ respectively represent the magnitudes of the in-phase and quadrature components of the error, and in which the superscript T denotes the operation of transposition. Sutton and Elliott [13, 14] suggested that the update of coefficient w_q of the controller, governing the qth in-phase component of the command signal could be performed by using the gradient descent algorithm

$$w_q(k+1) = w_q(k) - \alpha\, \partial J/\partial w_q, \tag{6}$$

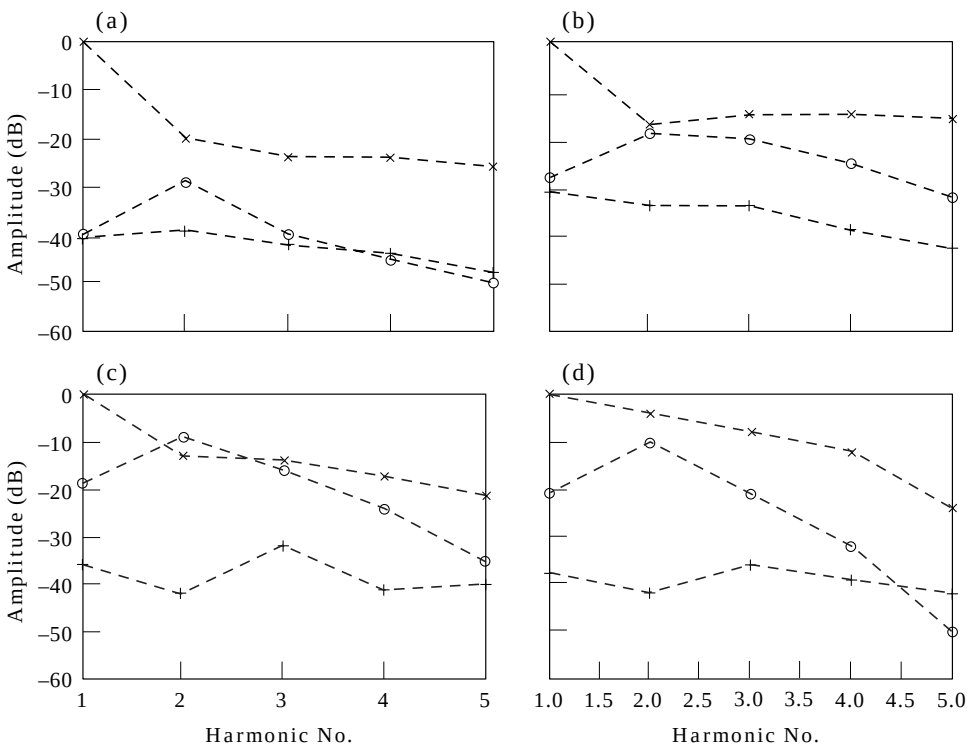

Figure 7. Harmonic contents of the acoustic pressure at the microphone location when the subsonic source is acting alone (×), for optimal manual control of the fundamental (○) and for optimal manual control of the fundamental and of the first four harmonics (+) of this signal. For comparison, the amplitude (before control) of the fundamental was set to 0 dB. (a) $f_0 = 35$ Hz; (b) $f_0 = 45$ Hz; (c) $f_0 = 60$ Hz; (d) $f_0 = 100$ Hz.

in which α is a real convergence coefficient. A similar equation also holds for the update of coefficient v_q, governing the qth quadrature component. The partial derivatives of J with respect to coefficient w_q can be written as [13, 14]

$$\frac{\partial J}{\partial w_q} \cong \frac{a_0}{2}\frac{\partial a_0}{\partial w_q} + \sum_{p=1}^{N} a_p \frac{\partial a_p}{\partial w_q} + \sum_{p=1}^{N} b_p \frac{\partial b_p}{\partial w_q}. \tag{7}$$

Physically, the partial derivative $\partial a_p/\partial w_q$ represents the sensitivity of the pth in-phase harmonic component of the Fourier transform of $e(t)$ to the weight of the qth in-phase harmonic component of the controller output, whereas the partial derivative $\partial b_p/\partial w_q$ represents the sensitivity of the pth quadrature harmonic component of the Fourier transform of $e(t)$ to the weight of the qth in-phase harmonic component of the controller output. The implementation of the gradient descent algorithm clearly requires a model of the non-linear plant under control, to allow the evaluation of the four sets of partial derivatives $\partial a_p/\partial w_q$, $\partial b_p/\partial w_q$, $\partial a_p/\partial v_q$ and $\partial b_p/\partial v_q$, the last two sets of partial derivatives being necessary for the update of coefficients v_q. These partial derivatives can for convenience be arranged in a single $(2N \times 2N)$ matrix of sensitivity $\mathbf{S}$ with real coefficients, defined as

$$\begin{bmatrix} \partial \mathbf{a} \\ \partial \mathbf{b} \end{bmatrix} = \underbrace{\begin{bmatrix} (\mathbf{S}_{\mathbf{aw}}) & (\mathbf{S}_{\mathbf{av}}) \\ (\mathbf{S}_{\mathbf{bw}}) & (\mathbf{S}_{\mathbf{bv}}) \end{bmatrix}}_{\mathbf{S}} \begin{bmatrix} \partial \mathbf{w} \\ \partial \mathbf{v} \end{bmatrix}, \tag{8}$$

where $\mathbf{S}_{\mathbf{aw}} = (\partial \mathbf{a}/\partial \mathbf{w})$, $\mathbf{S}_{\mathbf{av}} = (\partial \mathbf{a}/\partial \mathbf{v})$, $\mathbf{S}_{\mathbf{bw}} = (\partial \mathbf{b}/\partial \mathbf{w})$ and $\mathbf{S}_{\mathbf{bv}} = (\partial \mathbf{b}/\partial \mathbf{v})$ are four $(N \times N)$ matrices of sensitivity. Should the system under control be linear, matrices of sensitivity would become diagonal, since, for example, the pth harmonic component of the Fourier transform of $e(t)$ is only sensitive to changes in the pth harmonic component of the controller output. In the linear case, matrices of sensitivity are diagonal and related by equations [13, 14]

$$\mathbf{S}_{\mathbf{aw}} = \mathbf{S}_{\mathbf{bv}} \qquad \text{and} \qquad \mathbf{S}_{\mathbf{av}} = -\mathbf{S}_{\mathbf{bw}}. \tag{9}$$

For the non-linear case, the computational cost associated with the implementation of the harmonic controller can be evaluated as follows, upon assuming once again that the Fourier decomposition of the error signal is limited to N in-phase and N quadrature components and that the control signal is also limited to N in-phase and N quadrature components, so that matrices of sensitivity are square. According to equation (8), the update of the $2N$ controller coefficients necessitates the computation of four $(N \times N)$ matrices of sensitivity with real coefficients, i.e., the computation of $4N^2$ values: the amount of coefficients to evaluate is proportional to the square of the controller size. Because of the non-linearity of the plant, these coefficients moreover depend on the operating point, and must ideally be re-evaluated after each iteration of the controller. True harmonic control can therefore have a high computational cost. The concept of decentralized control, originally introduced for feedforward active control in multichannel, linear systems [18] can be an efficient way for reducing this

computational cost. This concept can be explained as follows, with reference to Figure 8. In centralized control [Figure 8(a)], the part of the controller driving each harmonic component in the control signal $u(t)$ is adjusted in response to the full harmonic contents ofthe error signal $e(t)$, as shown by equation (7). Decentralized control [Figure 8(b)] replaces the fully coupled contoller by a number of smaller adaptive controllers implemented independently, with each individual controller driving subsets of harmonic contents of $u(t)$, to minimize the sum of squared outputs of subsets of the harmonic contents of the error signal. The limit of this concept is when the nth harmonic component of $u(t)$ is adjusted to minimize only the nth harmonic component of $e(t)$. The reduction in computational cost achieved when replacing the centralized controller by its decentralized version can be estimated as follows. Decentralized feedforward control in a non-linear plant with N harmonic components in both the secondary source input and in the error signal requires the evaluation of the square matrix $\mathbf{S}$ defined as

$$\hat{\mathbf{S}} = \begin{bmatrix} (\hat{\mathbf{S}}_{aw}) & (\hat{\mathbf{S}}_{av}) \\ (\hat{\mathbf{S}}_{bw}) & (\hat{\mathbf{S}}_{bv}) \end{bmatrix}, \tag{10}$$

where for example the square diagonal matrix $\hat{\mathbf{S}}_{aw}$ is the matrix formed of the main diagonal of matrix $\mathbf{S}_{aw}$. Each update of the $2N(w_1, \ldots, w_n; v_1, \ldots, v_n)$ controller weights therefore only necessitates the evaluation of $4N$ real coefficients, when the centralized approach was demonstrated to require, for the same controller size, the evaluation of $4N^2$ real coefficients. Note that when the non-linearity of the plant under control is weak enough so that this plant can be accurately represented by a linear model, the number of coefficients to evaluate is even reduced, since

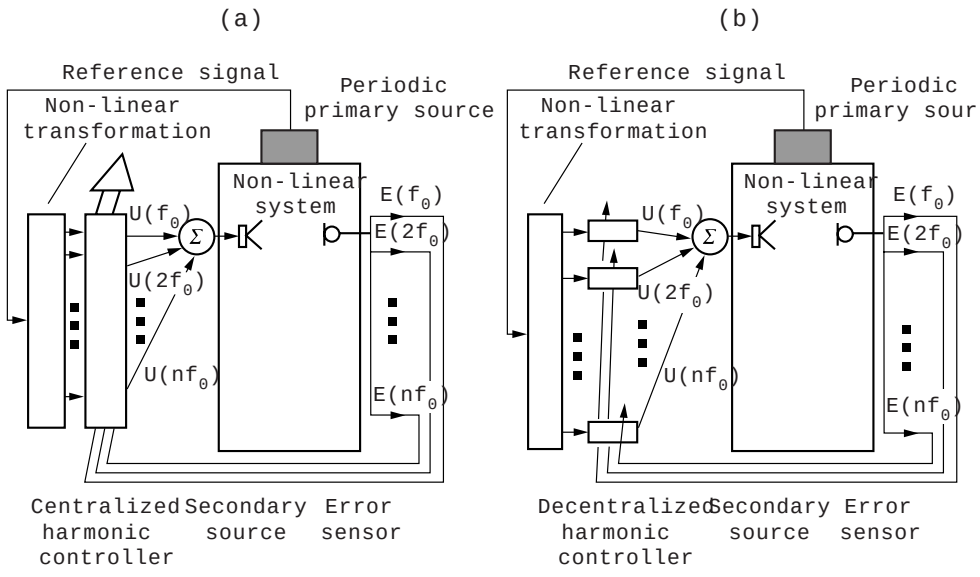

Figure 8. Illustration of the concepts of centralized (a) and decentralized (b) control applied to the control of a periodic disturbance of fundamental frequency f_0 in a single channel feedforward, non-linear system.

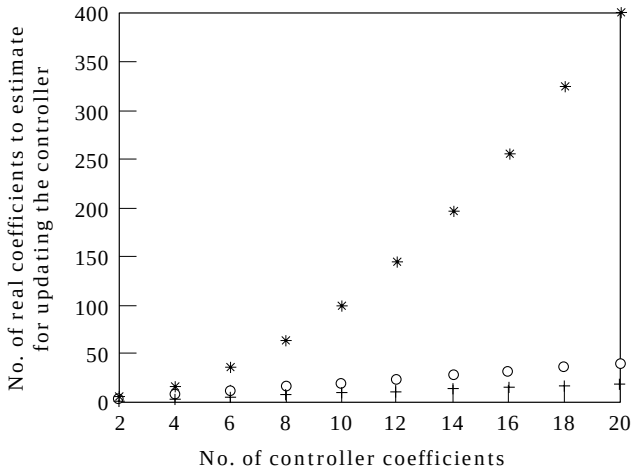

Figure 9. Single channel feedforward control in non-linear systems: number of coefficients to evaluate for updating the controller. ∗, centralized controller; ○, decentralized controller; +, decentralized controller for a weakly non-linear plant.

the matrix $\hat{\mathbf{S}}$ in equation (10) can be simplified by using equation (9), so that the number of real coefficients to evaluate reduces to $2N$. Figure 9 illustrates the computational power required to implement a fully coupled harmonic controller, to implement a decentralized controller and to implement a simplified version of the decentralized controller, designed for controlling a weakly non-linear system. If the decentralized approach is efficient in reducing the computational power required to implement the controller, no evidence *a priori* exists that this controller is likely to converge toward the optimal solution. A general condition of convergence of the decentralized controller is established in the Appendix. To summarize the result achieved, a necessary and sufficient condition for convergence of a decentralized procedure based on a steepest descent algorithm with slow convergence is that the eigenvalues of matrix $\mathbf{M}(k) = \mathbf{S}^{\mathrm{T}}(k)\hat{\mathbf{S}}(k) + \hat{\mathbf{S}}^{\mathrm{T}}(k)\mathbf{S}(k)$, in which the superscript T denotes matrix transposition, are all positive at each step of adaptation of the controller.

The convergence of the decentralized controller in the particular case where it drives the subsonic source is now analyzed. As shown above, this analysis requires the evaluation of the coefficient of matrix of sensitivity $\mathbf{S}$ at the various stages of the control procedure which was measured as explained in the following section.

5. EXPERIMENTAL ANALYSIS OF THE HARMONIC CONTROLLER

According to equation (8), matrix $\mathbf{S}(k)$ can be split into four $(N \times N)$ matrices $\mathbf{S}_{\mathbf{aw}}(k)$, $\mathbf{S}_{\mathbf{av}}(k)$, $\mathbf{S}_{\mathbf{bw}}(k)$ and $\mathbf{S}_{\mathbf{bv}}(k)$. As already explained, the ith line, jth column real coefficient $s_{aw,ij}$ of matrix $\mathbf{S}_{\mathbf{aw}}$ represents the sensitivity of the ith in-phase harmonic component of the error acoustic pressure to changes in the jth in-phase harmonic

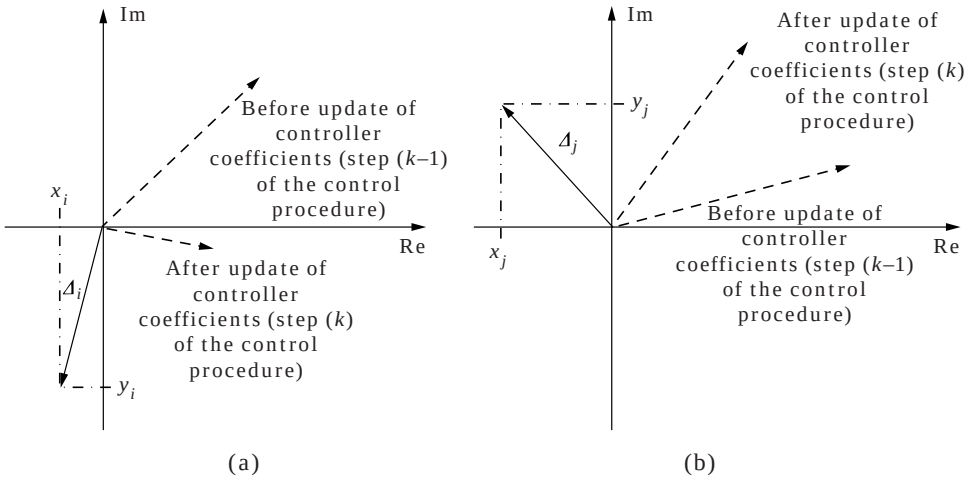

Figure 10. Estimation of the coefficients of the matrix of sensitivity. (a) Illustration in the complex plane of the characteristics of harmonic i component of the error signal picked up by the monitor microphone, before and after a change in the characteristics of harmonic j component in the signal driving the subsonic source; vector $\Delta_i = (x_i, y_i)$ is the difference between the two vectors. (b) Illustration in the complex plane of the characteristics of harmonic j component of the signal driving the subsonic source before and after a change in this harmonic component; vector $\Delta_j = (x_j, y_j)$ is the difference between the two previous vectors.

component of the signal driving the subsonic source. With reference to Figure 10, this coefficient can be estimated as

$$s_{aw,ij} = \Delta x_i / \Delta x_j \tag{11}$$

in which $\Delta x_i = a_i(k) - a_i(k-1)$ is the difference in the ith in-phase components of the error signal between steps (k) and $(k-1)$ of adaptation of the controller and $\Delta x_j = w_j(k) - w_j(k-1)$ is the difference in the jth in-phase components of the signal driving the subsonic source between steps (k) and $(k-1)$ of adaptation of the controller. The coefficients of the matrices $\mathbf{S_{av}}$, $\mathbf{S_{bw}}$ and $\mathbf{S_{bv}}$ can be estimated by using a similar approach, and referring to Figure 10, one can write

$$s_{av,ij} = \frac{\Delta x_i}{\Delta y_j}, \qquad s_{bw,ij} = \frac{\Delta y_i}{\Delta x_j} \qquad \text{and} \qquad s_{bv,ij} = \frac{\Delta y_i}{\Delta y_j}. \tag{12}$$

The estimation of the coefficients of the matrices of sensitivity was performed by using the manual version of the harmonic controller described in section 3. With reference to Figure 11, the control procedure consisted in manually adjusting the magnitudes w_i of the in-phase components and the magnitudes v_i of the quadrature components of signal $u(t)$ so that the rms value of the signal picked up by a microphone located close to the secondary source output was reduced, the final aim being the minimization of this signal. The fundamental and the first four harmonics of signal $u(t)$ were controlled, which was experimentally demonstrated in section 3 to be sufficient to guarantee attenuation larger than 30 dB at the microphone location. The coefficients of matrix $\mathbf{S}$ were estimated as follows. The 10 weights $[w_1, w_2, \ldots, w_5; v_1, v_2, \ldots, v_5]$ of the signal $u(t)$ were manually adjusted, which corresponded to one step of manual adaptation of the controller. The

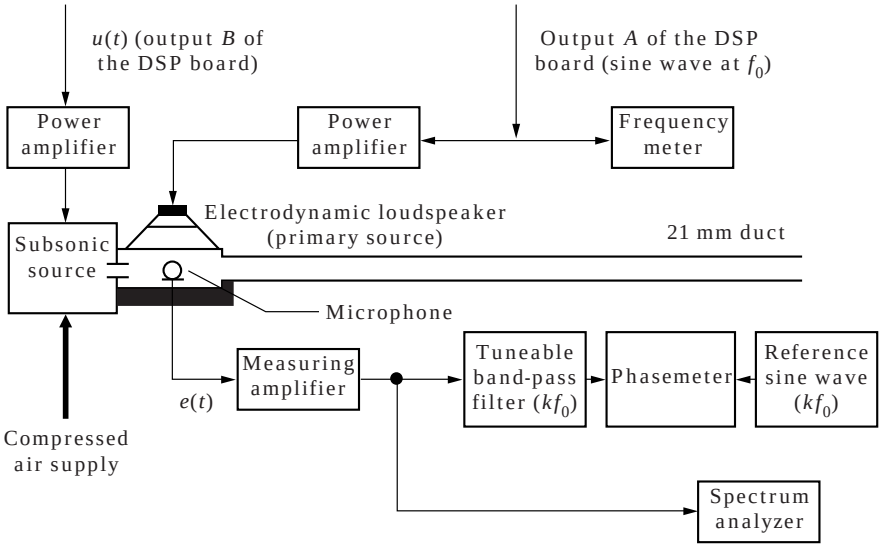

Figure 11. Experimental set-up for the experimental determination of the coefficients of the matrix of senstivity. The generation of signal $u(t)$ and of the signal driving the primary source was performed by using a dual channel signal processing board, as shown in Figure 3.

follwing quantities were estimated, both *before any change* in signal $u(t)$ and *after the modification* of the 10 weights $[w_1, w_2, \ldots, w_5; v_1, v_2, \ldots, v_5]$ of signal $u(t)$: the magnitude of the in-phase $[w_1, w_2, \ldots, w_5]$ and quadrature $[v_1, v_2, \ldots, v_5]$ components of signal $u(t)$; these magnitudes were directly read on the control panel of the algorithm implementing the manual harmonic controller; the magnitude of the in-phase $[a_1, a_2, \ldots, a_5]$ and quadrature $[b_1, b_2, \ldots, b_5]$ components of the error signal $e(t)$.

The in-phase a_n and quadrature b_n components of the nth harmonic of signal $e(t)$ were estimated as follows, with reference again to Figure 11. The amplitude C_n of this nth harmonic component was first measured, by using a spectrum analyzer. Its phase φ_n was then measured: the harmonic n component of the error signal was isolated by using a tuneable second-order bandpass filter and its phase was compared to the phase of a reference sine signal also at frequency (nf_0). Note that the phase of the harmonic n component of the error signal was not altered by the second order bandpass filter, since such a filter introduces zero phase shift at the centre frequency [19]. The values of a_n and b_n were then computed from C_n and φ_n by using the equation

$$a_n \cos(n\omega_0 t) + b_n \sin(n\omega_0 t) = C_n \sin(n\omega_0 t + \varphi_n) \tag{13}$$

where $a_n = C_n \sin \varphi_n$ and $b_n = C_n \cos \varphi_n$. From the measured values, the coefficients of matrix **S** were then estimated, by using equations (11) and (12). The experimental determination of the coefficients of matrix **S** was performed at the same fundamental frequencies f_0 as in section 3, i.e., 35, 45, 60 and 100 Hz, and for various plenum pressures. For each frequency, the matrix of sensitivity was evaluated at five steps during the active control procedure. Coefficients of matrix **S** were, for each of the frequencies considered, plotted versus the adaptation step.

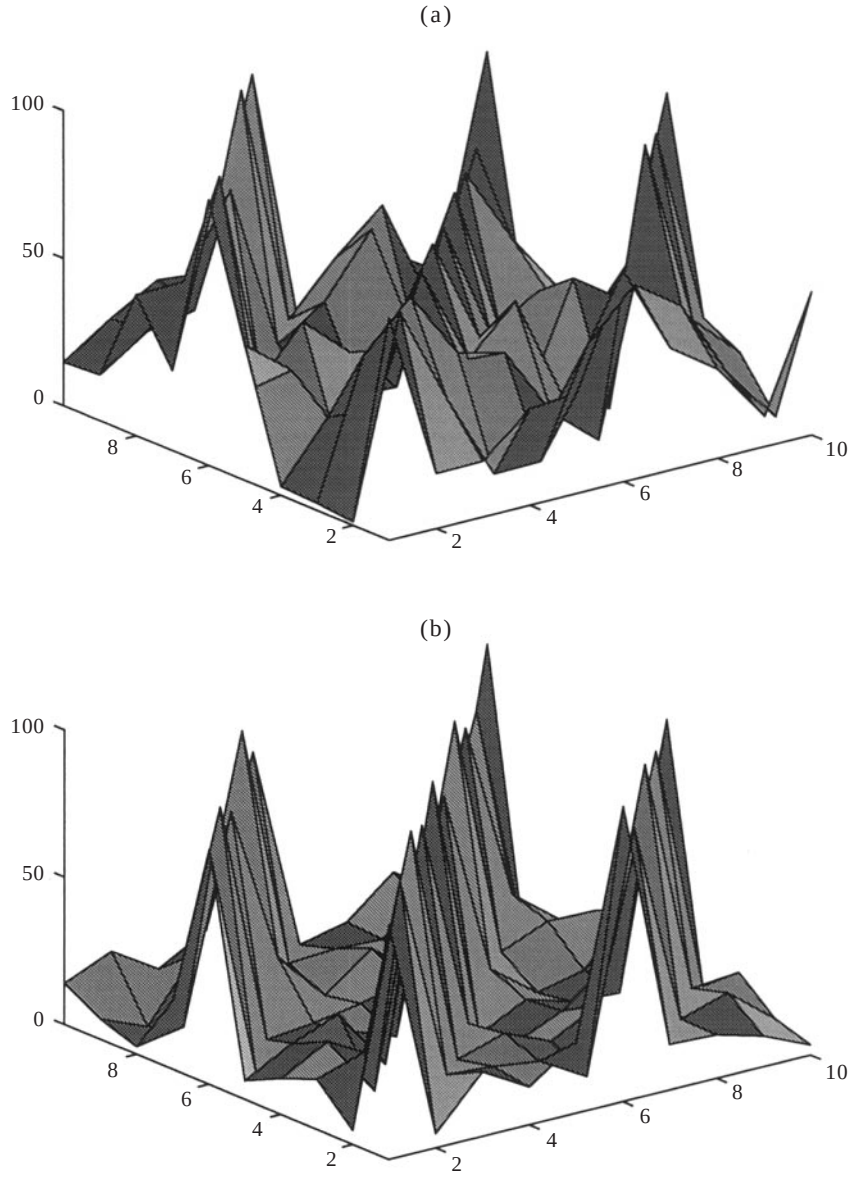

Figure 12. Plot of absolute value of the coefficients of the matrices of sensitivity **S** at steps 1 and 5 of the control procedure, in % of the largest coefficient of the matrix. Experimental conditions: $f_0 = 45$ Hz, plenum pressure was 59 Pa above the atmospheric pressure. (a) First step of manual update of controller coefficients; (b) fifth step of update of controller coefficients.

A typical result is given in Figure 12, for $f_0 = 45$ Hz, at the first ($k = 1$) and the last ($k = 5$) steps of manual adaptation of the controller. Results achieved for other frequencies were quite similar. At the very beginning of the manual control procedure, the system is clearly non-linear, since the off-diagonal terms of the submatrices $\mathbf{S}_{aw}$, $\mathbf{S}_{av}$, $\mathbf{S}_{bw}$ and $\mathbf{S}_{bv}$ are far from being negligible. As the step of adaptation of the controller increases, the structure of matrices **S** converge to the

structure of matrices $\mathbf{S}$ for a linear system with the submatrices $\mathbf{S}_{aw}$, $\mathbf{S}_{av}$, $\mathbf{S}_{bw}$ and $\mathbf{S}_{bv}$ forming matrix $\mathbf{S}$ becoming almost diagonal and related by the expressions

$$\mathbf{S}_{aw} \cong \mathbf{S}_{bv} \qquad \text{and} \qquad \mathbf{S}_{av} \cong -\mathbf{S}_{bw}, \tag{14}$$

since, for the four frequencies considered, the difference between the elements of $\hat{\mathbf{S}}_{aw}$ and of $\hat{\mathbf{S}}_{bv}$ never exceeded 12%, whereas the difference between the elements of $\hat{\mathbf{S}}_{av}$ and $-\hat{\mathbf{S}}_{bw}$ never exceeded 19%. This result is consistent with the fundamental equation of subsonic sources [equation (1)] and with the experimental results of Figure 4. The linearity of the sound emission process was indeed proved to increase as the acoustic pressure at the source output decreases, which leads matrices $\mathbf{S}_{aw}$, $\mathbf{S}_{av}$, $\mathbf{S}_{bw}$ and $\mathbf{S}_{bv}$ to be closer and closer to purely diagonal matrices as k increases. Should the subsonic source be perfectly linear, these matrices would be purely diagonal. The magnitude of the off-diagonals coefficients of matrices $\mathbf{S}$ at step 5 of the control procedure, when the controller is assumed to be converged, can hence be seen as a measurement of the subsonic source residual non-linear behaviour. The stability of the decentralized controller was then assessed. Matrix $\hat{\mathbf{S}}$ was taken to be the average linear approximation of matrix $\mathbf{S}$ and the matrix $\mathbf{M}(k) = \mathbf{S}^{\mathrm{T}}(k)\hat{\mathbf{S}}(k) + \hat{\mathbf{S}}^{\mathrm{T}}(k)\mathbf{S}(k)$ was computed for each iteration of the controller and at each frequency. The eigenvalues were then calculated for the matrix $\mathbf{M}$ at steps 1 and 5 of adaptation of the controller. The computed eigenvalues were all real, which was expected since matrices $\mathbf{M}$ are symmetric. At the beginning of the control procedure ($k = 1$) some eigenvalues were found, for each of the frequencies f_0 and each plenum pressure considered, to be *negative*. The situation was different at step 5 of the control procedure, since *all* the computed eigenvalues were in this case found to be *positive*. If the system under control were linear, the eigenvalues of matrix $\mathbf{M}$ would all be positive. When the controller has reached its converged state, the subsonic source is only weakly non-linear, and matrix $\mathbf{M}(5)$ can be considered to differ from matrix $\mathbf{M}$ for a linear system by a small amount, which intuitively suggests that the eigenvalues of matrix $\mathbf{M}(5)$ should be positive.

In view of the theoretical analysis carried out in the Appendix, that establishes a necessary and sufficient condition of convergence of the controller, the above experimental results demonstrate that the critical moment of the convergence of the decentralized controller is the very beginning of the control procedure: should divergence happen, the phenomenon would take place immediately. This suggests that it is necessary to "help" the decentralized controller in its task, at least at the beginning of the control procedure. The following control strategy can therefore be suggested, upon assuming a sinusoidal primary sound field: (i) control of the fundamental frequency only of the error signal, by driving the subsonic source with a sinusoidal signal $u(t)$; (ii) when the amplitude of the fundamental has reached a minimum, start the decentalized control procedure. This control strategy would guarantee the decentralized controller to operate in optimal conditions, since this controller would have to control a weakly non-linear system.

6. SHAPE OF THE ERROR SURFACE

The non-linear behaviour of the subsonic source causes a further problem: unlike in the linear case, the error surface is not guaranteed to be a quadratic or

even convex function of the controller coefficients, and it is possible for this surface to exhibit several minima. In other words, even if convergence of the controller is ensured, a risk exists of being trapped in a local minimum of the error surface and of failing to detect the global minimum. The analytic determination of the equation governing the shape of the error surface is difficult. The shape of the error surface when driving the primary source with a pure tone at f_0 was hence investigated experimentally. As previously explained, efficient active control with the subsonic source requires the control of 10 parameters, which is also the dimension of the error surface. The experimental determination of this surface may thus be time consuming and tedious. It was therefore decided to control the fundamental of signal $u(t)$ only or, in other words, to drive the subsonic source with a sinusoidal signal. This procedure is consistent with the control strategy outlined at the end of the previous section. The experimental set-up used to estimate the shape of the error surface is illustrated in Figure 13. The primary source was driven with a sinusoidal signal at f_0. The control of the magnitude of the in-phase and quadrature components of the sinusoidal signal $u(t)$ was replaced by the control of the amplitude C_1 and of the phase φ_1 of this signal. To reduce the dimension of the error surface, the phase φ_1 was adjusted, prior to control, to a value leading to optimal control at the error microphone. The problem hence became one dimensional, since the only parameter that was adjusted was the amplitude C_1 of signal $u(t)$. By making the amplitude C_1 vary, sinusoidal modulations of various amplitude of the valve were achieved. A spectrum analyzer was used to measure the magnitude of the fundamental component of the error signal $e(t)$. Experiments were again conducted at 35, 45, 60 and 100 Hz and for each single frequency, experiments were carred out at two amplitudes of the primary acoustic field (and hence at two different plenum pressures). The magnitude of the fundamental component of the error signal $e(t)$ versus the amplitude of the sinusoidal modulation of the throat area is illustrated in Figure 14, for $f_0 = 45$ Hz. The fundamental component of the error signal is shown to decrease as the modulation of the valve increases and exhibits a single, global

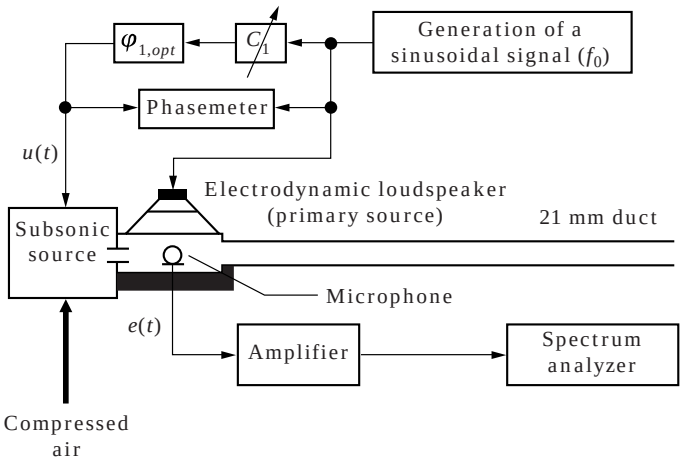

Figure 13. Experimental set-up to measure the shape of the error surface.

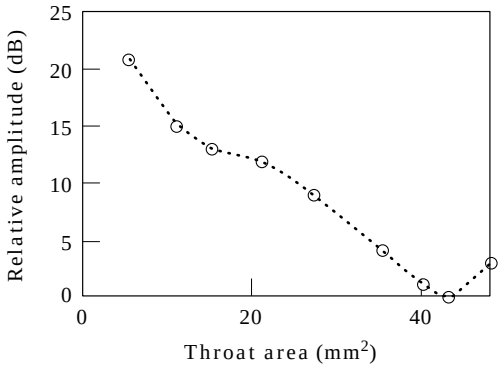

Figure 14. Relative amplitudes $A_{1r,k}$ of the fundamental and relative amplitudes $A_{ir,k}$ of the first three harmonics of the error signal for various sinusoidal modulations of the throat area. Primary source was driven with a sinusoidal signal at 45 Hz and the plenum pressure was 197 Pa above the atmospheric pressure.

minimum. The optimal modulation of the throat area, defined as the sinusoidal modulation for which optimal control is achieved, depends on the experimental conditions: i.e., on the ratio between the plenum pressure and the amplitude of the primary sound field. As this ratio increases, optimal modulation is achieved for relatively small excursions of the slider: the subsonic source behaves quite linearly but is inefficient. To increase source efficiency it is important to work with realtively small plenum pressure excess. In this case optimal modulation of the throat area implies large excursions of the slider and the source then behaves non-linearly. If the plenum pressure excess is below a given value, the volume velocity produced by the subsonic source is, even for full modulation of the valve, not large enough to compensate for the volume velocity derived by the primary source and optimal active control is no longer possible. The important conclusion from the experimental results is that, for the fundamental frequency, the error signal exhibits a single minimum versus the modulation area. This shows that the control strategy outlined in the previous section should avoid the risk of leaving the controller trapped in a local minimum.

The shape of the error surface was then estimated. For each frequency, the sum of the squared amplitudes of the fundamental and of the harmonic components of the error signal was computed for various amplitudes of modulation of the throat area. For convenience, this sum was related to its minimum value A_{min}, so that the following non-dimensional cost function was defined:

$$\text{Cost function } (k) = 10 \log \left[\left(\sum_{i=1}^{4} A_{i,k}^2 \right) \Big/ A_{min} \right]. \tag{15}$$

This cost function is illustrated, for the four frequencies considered, in Figure 15. Because of the non-linear behaviour of the subsonic source, the cost function is not quadratic. For the experimental conditions considered, it however exhibits a single global minimum; i.e., it is convex. This result suggests that provided the controller is stable, it should converge toward the optimal solution. From the

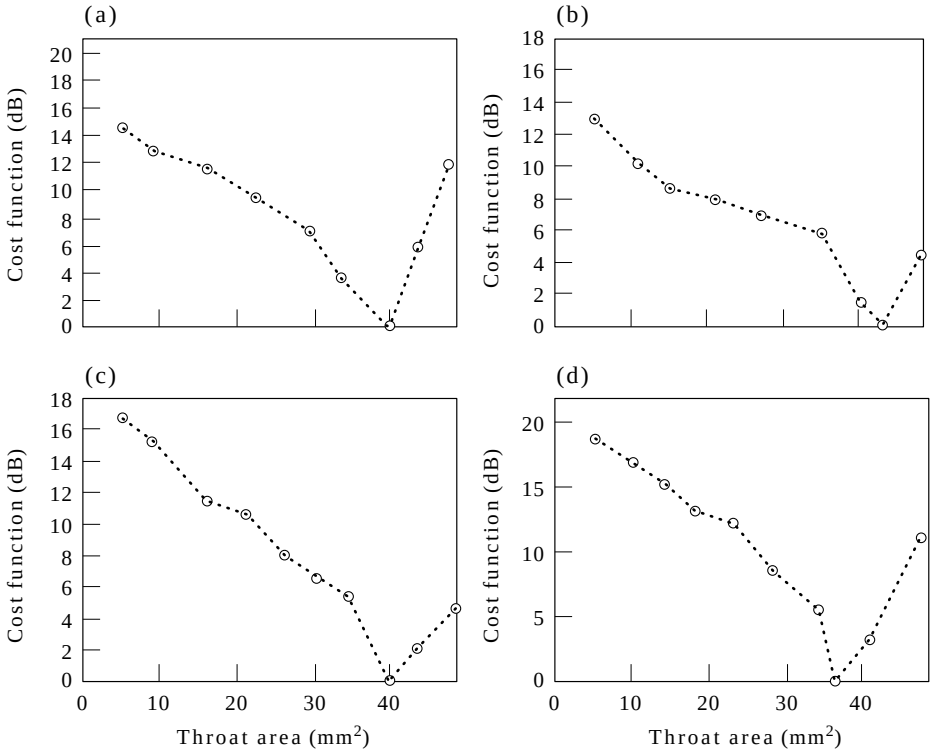

Figure 15. Error surface, computed according to equation (15), for various sinusoidal modulations of the throat area. Primary electrodynamic loudspeaker was driven with a sinusoidal signal at f_0. (a) $f_0 = 35$ Hz, $p_{pl} = p_{atm} + 57$ Pa; (b) $f_0 = 45$ Hz, $p_{pl} = p_{atm} + 82$ Pa; (c) $f_0 = 60$ Hz, $p_{pl} = p_{atm} + 44$ Pa; (d) $f_0 = 100$ Hz, $p_{pl} = p_{atm} + 95$ Pa.

experimental results it seems that the cost function is more abrupt for modulations of the throat larger than the optimal modulation than for modulations smaller than this optimal modulation. This can be explained by noting that the subsonic source non-linear behaviour—and hence the harmonic contents at its output—increases with the modulation of the throat area. This result suggests that the first step of the control strategy outlined in the previous section—control of the error signal by adjusting only the fundamental frequency only of the error signal—should start while the valve of the subsonic source is fully modulated. This could be expected, according to the results above, to accelerate the convergence of the controller.

Finally, it is important to note that the above discussion is based on experimental results that are far from being exhaustive: experiments carreid out for other frequencies and other plenum pressures may possibly lead to different conclusions. It is also important to bear in mind that the shape of the error surface was measured only as a function of one parameter. In other words, only a very limited portion of the error surface was investigated. From our results it is difficult to reach any firm conclusions about the shape of the whole error surface. If, however, the automatic harmonic controller leads to attenuations at the error microphone similar to those achieved with the manual version of this controller,

it will be concluded that the controller has converged toward the optimal solution; if not it will be concluded that the controller is probably trapped in a local minimum. Should such a situation occur, simulated annealing [20], tabu search [21] or genetic methods [22] could be implemented to reduce the risk of remaining trapped in a local minimum.

7. IMPLEMENTATION OF AN AUTOMATIC HARMONIC CONTROLLER

An automatic version of the decentralized harmonic controller was also implemented. From the above results it was decided to control only five harmonics of the signal driving the subsonic source and to limit the Fourier decomposition of the error signal also to five harmonic components. Section 5 showed how quite a simple model, in which sensitivity arrays were purely diagonal, could be used to model the behaviour of the subsonic source while ensuring the convergence of the control algorithm. The implementation of an automatic version of the harmonic controller clearly necessitates the evaluation of the coefficients of four diagonal arrays of sensitivity $\hat{\mathbf{S}}_{aw}$, $\hat{\mathbf{S}}_{bw}$, $\hat{\mathbf{S}}_{av}$ and $\hat{\mathbf{S}}_{bv}$. In principle, these coefficients need to be re-evaluated after each iteration of the controller, because of the non-linearity of the plant under control. The literature however describes at least two examples [13, 14] in which a static model of the plant under control was successfully used to perform harmonic active control in a non-linear system. This simplified procedure is justified by the fact that the steepest descent algorithm is robust and can, as in the linear case, be expected to tolerate some error in the plant model.

The algorithm for harmonic control described in section 5, in which the fundamental component is adjusted first, is such that the decentralized control procedure starts while the source only exhibits a residual non-linear behaviour. The coefficients of the matrices of sensivity can therefore be expected to be almost independent on the operating point, which suggests that a static model can be used for the plant. The results of the manual harmonic control procedure described in section 5 were used to fix the coefficients of the sensitivity array $\hat{\mathbf{S}}_S$ (in which subscript **S** stands for static). These coefficients were chosen equal to their value at the very end of the manual control procedure, when the error signal picked up by the monitor microphone has reached a minimum value. For example, the values corresponding to the diagonals of matrix **S** given by Figure 12 at the fifth stp of adaptation of the controller were chosen for the sensitivity arrays at 45 Hz. Since the sensitivity arrays are approximately related by equation (14), the elements of matrix $\hat{\mathbf{S}}_{S,BV}$ were moreover chosen to be equal to the elements of matrix $\hat{\mathbf{S}}_{S,AW}$ and the elements of matrix $\hat{\mathbf{S}}_{S,BW}$ were chosen to be equal (and opposite) to the elements of matrix $\hat{\mathbf{S}}_{S,AV}$. In other words, a purely linear model was used to represent the plant under control.

A Texas Instruments TMS320C25 signal processing board was used to implement the harmonic controller. The assembler routine that was written can be split in three blocks. The first block generated a cosine signal, used to drive the primary source and generated the first four harmonic components of this cosine signal, used to feed (together with the fundamental) the harmonic

controller. This internal generation avoided problems of synchronization. The successive values of the fundamental and of the first four harmonic components of a cosine signal were pre-computed, and the resulting values were stored in a table placed in the memory of the signal processing board. The symmetry of the cosine function was used to reduce the amount of stored data, and only the values corresponding to a quarter of a period of both the fundamental and the first four harmonics were stored. The second block of the routine was devoted to the computation of the digital Fourier transform of the error signal, measured by the monitor microphone. This Fourier transform was computed by using data corresponding to a full period of the error signal. Since the subsonic actuator generates no subharmonics [1], the fundamental frequency of the error signal was equal to the fundamental frequency of the signals produced by both the electrodynamic loudspeaker and the subsonic source. A full period of the signal derived by these devices corresponding to 240 points, the computation of the Fourier transform of the error signal was based on 240 successive values of this signal. A radix-2 fast Fourier transform algorithm was used to compute this transform. An important feature of radix-2 algorithms is that they are faster and more accurate when the length of the input sequence is a power of two. To meet this requirement, 16 zeros were added to the 240 measured values of the error signal. The third part of the routine computed the command signal $u(t)$, by using equation (2) and updated coefficients w_i and v_i of the controller, by using equations (6) and (7). The coefficients of the sensitivity array $\hat{\mathbf{S}}_S$ for a given frequency f_0 were stored on the hard disk of the P.C. and were sent to the memory of the signal processing board at the very beginning of the control procedure. In an initial phase of control only the fundamental of the error signal was controlled. The adaptive adjustment of coefficients started when the valve of the subsonic source was fully modulated, which corresponded to the following initial conditions: $w_1 = 1$, $v_1 = 0$. This initial condition was proved in section 6 to limit the risk of remaining trapped in a local minimum of the error surface. As soon as the fundamental of the error signal has reached a minimum value, the control of the harmonic components of signal $u(t)$ can start. This was achieved manually by monitoring the level L_f of the fundamental of the error signal and by starting the control of the harmonic components of $u(t)$ when level L_f reached its minimum value. This procedure gave the operator the possibility of starting the control of the harmonic components of $u(t)$ while the fundamental of $e(t)$ has not yet reached its minimum value, which was useful in investigating the robustness of the control algorithm.

The block diagram of the experimental set-up that was used for performing automatic active control is illustrated in Figure 16. An electronic fuse was placed at the output of the d.c. power amplifier driving the subsonic source, to protect the electrodynamic shaker against a possible divergence of the automatic controller. Automatic active control experiments were conducted for sinusoidal primary sound fields. A first set of experiments was conducted, at the same frequencies and for the same plenum pressures than for the manual control experiments of section 3. The results are presented in Figure 17. In each case, the controller was found to converge, which demonstrates that the linear model used to represent the plant under control was reasonably accurate. Other experiments

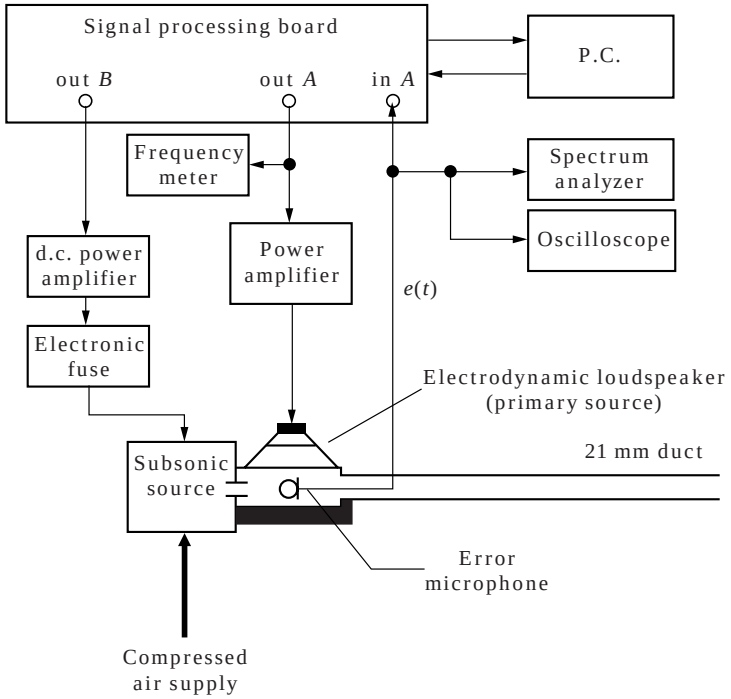

Figure 16. Experimental set-up for automatic active noise control experiments with the subsonic source.

were conducted for the same frequencies, but with other levels of the primary sound field and other plenum pressures. The controller was also found to converge in these cases, which shows that the sensitivity arrays can be considered to be independent of the source operating point, at least when the fundamental of the error signal has been cancelled out. As stated in the previous section, the algorithm that was implemented gave the operator the possibility of starting the harmonic control procedure when the fundamental of the error signal has not yet reached a minimum. Experiments were therefore conducted in which the harmonic control procedure started prematurely, i.e., before L_f had reached a minimum. In most cases, the controller failed to converge toward the optimal solution. This suggests that the simplified, linear model that was implemented to represent the plant under control is accurate only when the acoustic pressure at the subsonic source output is weak enough so that this source behaves weakly non-linearly. Figure 18 compares the harmonic contents at the microphone location measured when the automatic controller has reached its steady state with the results that were achieved in section 3, i.e., with the harmonic contents at the error microphone when (i) the subsonic source is acting alone, (ii) when manual control of the fundamental only is achieved, and (iii) when optimal manual harmonic control is performed. Broadly speaking, the harmonic contents achieved for automatic control was at least 10 dB below the harmonic contents measured for active control of the fundamental only. The harmonic contents achieved for automatic control was found to be very close to that achieved for manual harmonic control, which shows that the automatic

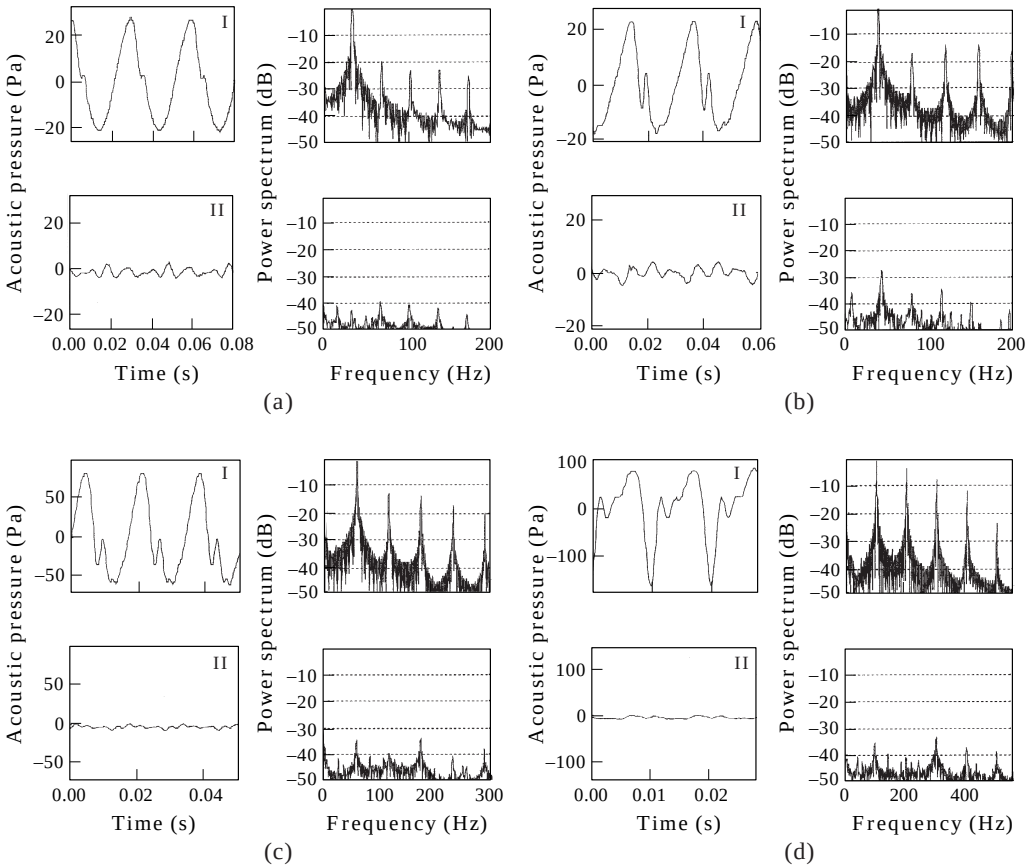

Figure 17. Acoustic pressure versus time and frequency at the microphone location, (I) when the subsonic source is acting alone and (II) for optimal automatic harmonic control of the fundamental and of the first four harmonic components. (a) $f_0 = 35$ Hz, $p_{pl} = p_{atm} + 53$ Pa; (b) $f_0 = 45$ Hz, $p_{pl} = p_{atm} + 68$ Pa; (c) $f_0 = 60$ Hz, $p_{pl} = p_{atm} + 134$ Pa; (d) $f_0 = 100$ Hz, $p_{pl} = p_{atm} + 274$ Pa.

controller was not trapped in a local minimum of the error surface. In the time domain, the rms sound pressure levels measured at the monitor microphone for automatic active control conditions were found, as in the case of manual harmonic control, to be around 25 dB below the sound pressure levels due to the primary sound field alone. This can be considered as a reasonable attenuation, especially if one takes into account the initial non-linear behaviour of the secondary actuator.

8. CONCLUSIONS

The objective of this paper was to analyze the possibility of integrating a subsonic electropneumatic acoustic generator in an active control system and to investigate the performance of this active noise control system in a practical situation. An analysis of this actuator was described in two companion papers [1, 2] and revealed that this actuator was efficient and robust, but non-linear. As expected from the theoretical analysis, however, controlling the fundamental

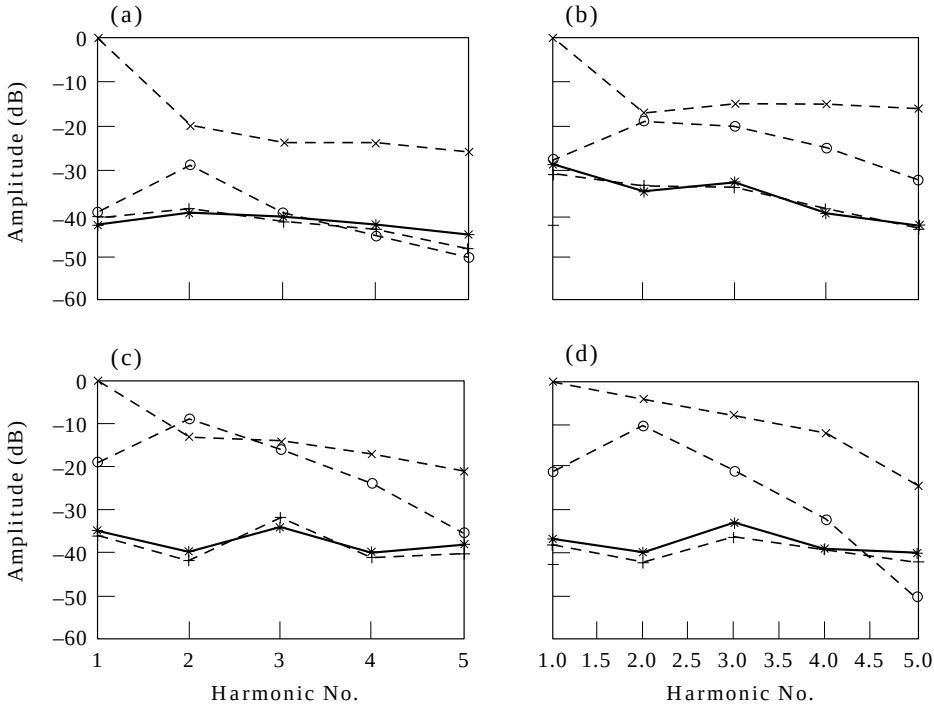

Figure 18. Harmonic contents of the acoustic pressure at the microphone location when the subsonic source is acting alone ($\times$), for optimal manual control of the fundamental ($\bigcirc$), for optimal manual control of the fundamental and of the first four harmonics ($+$) and for optimal control with the harmonic controller ($*$ and solid line). The amplitude of the fundamental before control was set to 0 dB. (a) $f_0 = 35$ Hz; (b) $f_0 = 45$ Hz; (c) $f_0 = 60$ Hz; (d) $f_0 = 100$ Hz. The results marked ($\times$), ($\bigcirc$) and ($+$) have already been presented in Figure 7.

frequency of the acoustic field at a location close to the subsonic source output was experimentally demonstrated to reduce its non-linear behaviour. For reasons associated mainly to the mechanical design of the subsonic source, the harmonic contents at its output was however not totally cancelled out, which limited the measured attenuation to about 18 dB. To increase these attenuations a manual harmonic controller was implemented, that controlled both the fundamental and the first four harmonics at the error microphone location. Measured attenuations were this time around 25 dB, which demonstrated the accuracy of the harmonic controller in attenuating tonal primary sound fields. The implementation of an automatic, adaptive harmonic controller was then considered. The implementation of a fully coupled harmonic controller was demonstrated to be likely to require large processing capacities, proportional to the square of the controller size. A simplified version of the fully coupled harmonic controller—the decentralized controller—was hence analyzed. The processing capacities required by the decentralized controller were shown to be proportional to the controller size. The convergence of the decentralized controller was discussed and a necessary and sufficient condition of convergence of this controller was established. Experiments carried out with a manual version of the harmonic controller revealed that this condition was fulfilled, at least when the fundamental component of the error

signal has been cancelled out. The non-linear behaviour of the subsonic source introduced a further difficulty, in that the error surface was not guaranteed to be quadratic. Experiments carried out to measure the shape of the error surface revealed that the presence of local minima in this surface was not likely, i.e., that this surface was convex. On the basis of the analysis of the behaviour of the subsonic source when performing active control, a particular control algorithm was suggested, in which the fundamental of the error signal was controlled first and in which the harmonic control started as soon as the amplitude of this fundamental component has reached a minimum value.

A dual channel signal processing board was used to implement this particular control algorithm. The algorithm controlled the fundamental and the first four harmonic components of the signal picked up by the monitor microphone, placed a few centimetres away from the secondary source output. A simplified, static, linear model was used to represent the non-linear plant under control, at least after the fundamental component of the error signal is cancelled out. This simple model was found to be accurate enough in representing the non-linear plant, since it guaranteed the convergence of the harmonic controller. Automatic control experiments were conducted at various frequencies. Attenuations at the error microphone were measured to be around 25 dB. The convergence of the controller was found to be unaffected by the level of the primary sound field and by the subsonic source plenum pressure. However, choosing a sensitivity array measured for a particular frequency for modelling the non-linear plant over a range of frequencies was found to destabilize the harmonic controller. The problem of the active control of a tonal primary field with a variable fundamental frequency is particularly interesting from a practical point of view, because the fundamental frequency of the quasi-periodic noise in vehicle exhaust pipes is not steady, since it depends directly on the engine rotational speed. A possible solution to guarantee the convergence of the controller in such a situation would be to re-evaluate the coefficients of the sensitivity array after each update of the controller coefficients.

REFERENCES

1. L. A. Blondel and S. J. Elliott 1998 *Journal of Sound and Vibration*. Eletropneumatic transducers as secondary actuators for active noise control, Part I: Theoretical analysis.
2. L. A. Blondel and S. J. Elliott 1998 *Journal of Sound and Vibration*. Electropneumatic transducers as secondary actuators for active noise control, Part II: Experimental analysis of the subsonic source.
3. A. Roure 1995 *Proceedings of the Conference on the Application of Active Control—CETIM*, *Senlis* (*France*), 3–8. Le contrôle actif, mais oui ça marche!
4. G. Guicking 1996 *Proceedings of ISMA* 21, *Leuven* (*Belgium*), 199–220. Active control of vibration and sound—an overview of the patent literature.
5. J. C. Burgess 1981 *Journal of the Acoustical Society of America* **70**, 715–726. Active adaptive sound control in a duct: a computer simulation.
6. P. A. Nelson and S. J. Elliott 1992 *Active Control of Sound*. London: Academic Press.
7. D. R. Birt 1991 *Journal of the Audio Engineering Society* **39**(4), 219–230. Nonlinearities in moving-coil loudspeakers with overhung voice coils.

8. W. KLIPPEL 1992 *Journal of the Audio Engineering Society* **40**(6), 483–496. Non-linear large-signal behaviour of electrodynamic loudspeakers at low frequencies.
9. C. I. BELTRAN 1995 *Proceedings of Active* '95, 837–848. Acoustic transducer nonlinearities and how they affect the performance of active noise control systems.
10. M. B. MOFFETT and A. E. CLARK 1991 *Journal of the Acoustical Society of America* **89**(3), 1448–1455. Characterization of Terfenol-D for magnetostrictive actuators.
11. W. KLIPPEL 1995 *Proceedings of Active* '95, 413–422. Active attenuation of nonlinear sound.
12. K. S. NARENDRA and K. PARTHASARATHY 1990 *IEEE Transactions on Neural Networks* **1**(1), 4–27. Identification and control of dynamical systems using neural networks.
13. T. J. SUTTON and S. J. ELLIOTT 1993 *Proceedings of the Institute of Acoustics* **15**, 775–784. Frequency and time domain controllers for the attenuation of vibration in nonlinear structural systems.
14. T. J. SUTTON and S. J. ELLIOTT 1995 *Journal of Vibration and Acoustics* **117**, 355–362. Active attenuation of periodic vibration in nonlinear systems using an adaptive harmonic controller.
15. W. B. CONOVER 1956 *Noise Control* **2**, 78–82. Fighting noise with noise.
16. D. R. MORGAN 1980 *IEEE Transactions on Acoustics, Speech and Signal Processing* **28**(4), 454–467. An analysis of multiple correlation cancellation loops with a filter in the auxiliary path.
17. S. J. ELLIOTT, C. C. BOUCHER and P. A. NELSON 1992 *IEEE Transactions on Signal Processing* **40**(5), 1041–1052. The behaviour of a multiple channel active control system.
18. S. J. ELLIOTT and C. C. BOUCHER 1994 *IEEE Transactions on Speech and Audio Processing* **2**(4), 521–530. Interaction between multiple feedforward active control systems.
19. J. MILLMAN and C. HALKIAS 1971 *Integrated Electronics*. Singapore: McGraw–Hill International.
20. S. KIRKPATRICK, C. D. GELATT and M. P. VECCHI 1983 *Science* **220**, 671–680. Optimisation by simulated annealing.
21. F. GLOVER 1986 *Computers & Operations Research* **5**, 533–549. Future paths for integer programming and links to artificial intelligence.
22. J. H. HOLLAND 1975 *Adaptation in Natural and Artificial Systems*. Ann Arbor, MI: The University of Michigan Press.
23. B. NOBLE and J. W. DANIEL 1977 *Applied Linear Algebra*, 2nd edition. New York: Prentice–Hall.
24. E. H. THOMPSON 1969 *Introduction to the Algebra of Matrices with Some Applications*. London: Hilger.

APPENDIX: THEORETICAL ANALYSIS OF THE CONVERGENCE OF THE DECENTRALIZED CONTROLLER

A condition of convergence of the decentralized controller when driving non-linear systems can be derived theoretically. Active noise control of tonal noise in non-linear systems is illustrated in Figure A1. Upon assuming the system is

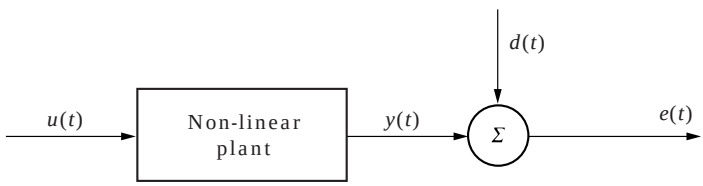

Figure A1. Active control of a periodic primary disturbance $d(t)$ in a non-linear system.

steady, the command signal $u(t)$ and the error signal $e(t)$ can respectively be written as

$$u(t) = \sum_{i=1}^{N} w_i \cos(i\omega_0 t) + v_i \sin(i\omega_0 t), \tag{A1}$$

$$e(t) = d(t) + y(t) = \sum_{i=0}^{N} a_i \cos(i\omega_0 t) + b_i \sin(i\omega_0 t). \tag{A2}$$

Upon assuming relatively weak changes in vectors $\mathbf{w}$ and $\mathbf{v}$ between steps $(k-1)$ and (k) of adaptation of the controller, coefficients of the Fourier transform of the error at step (k) can be written as

$$\begin{bmatrix} \mathbf{a}(k) \\ \mathbf{b}(k) \end{bmatrix} = \begin{bmatrix} \mathbf{a}(k-1) \\ \mathbf{b}(k-1) \end{bmatrix} + \mathbf{S}(k) \begin{bmatrix} \mathbf{w}(k) - \mathbf{w}(k-1) \\ \mathbf{v}(k) - \mathbf{v}(k-1) \end{bmatrix}, \tag{A3}$$

or

$$\mathbf{e}(k) = \mathbf{e}(k-1) + \mathbf{S}(k) \Delta \mathbf{u}(k), \tag{A4}$$

where

$$\mathbf{e}(k) = \begin{bmatrix} \mathbf{a}(k) \\ \mathbf{b}(k) \end{bmatrix} \quad \text{and} \quad \Delta \mathbf{u}(k) = \begin{bmatrix} \mathbf{w}(k) - \mathbf{w}(k-1) \\ \mathbf{v}(k) - \mathbf{v}(k-1) \end{bmatrix}.$$

Upon assuming that a steepest descent algorithm is used to adapt the coefficient of the decentralized controller, and that the decentralized matrix of convergence $\hat{\mathbf{S}}$ is re-evaluated after each update of the controller coefficients, so that $\hat{\mathbf{S}}(k) \neq \hat{\mathbf{S}}(k-1)$, then vector $\Delta \mathbf{u}(k)$ can be written as (if α is a real convergence coefficient [6])

$$\Delta \mathbf{u}(k) = -\alpha \hat{\mathbf{S}}^{\mathrm{H}}(k) \mathbf{e}(k-1) \quad \text{or} \quad \Delta \mathbf{u}(k) = -\alpha \hat{\mathbf{S}}^{\mathrm{T}}(k) \mathbf{e}(k-1), \tag{A5}$$

since the coefficients of matrix $\hat{\mathbf{S}}$ are real, so that the Hermitian transpose of this matrix is equal to its transpose. Combining equations (A4) and (A5) yields

$$\mathbf{e}(k) = [\mathbf{I} - \alpha \hat{\mathbf{S}}^{\mathrm{T}}(k) \mathbf{S}(k)] \mathbf{e}(k-1), \tag{A6}$$

where $\mathbf{I}$ is the identity matrix. The cost function at the kth step of adaptation is written [6]:

$$J(k) = \mathbf{e}^{\mathrm{T}}(k) \mathbf{e}(k), \tag{A7}$$

or, upon using equation (A6),

$$J(k) = \mathbf{e}^{\mathrm{T}}(k-1) [\mathbf{I} - \alpha \mathbf{S}^{\mathrm{T}}(k) \hat{\mathbf{S}}(k)] [\mathbf{I} - \alpha \hat{\mathbf{S}}^{\mathrm{T}}(k) \mathbf{S}(k)] \mathbf{e}(k-1). \tag{A8}$$

If slow adaptation of the controller coefficients is assumed, then it is reasonable to assume that

$$\alpha^2|\mathbf{S}^{\mathrm{T}}(k)\hat{\mathbf{S}}(k)\hat{\mathbf{S}}^{\mathrm{T}}(k)\mathbf{S}(k)| \ll \alpha|\mathbf{S}^{\mathrm{T}}(k)\hat{\mathbf{S}}(k)|, \tag{A9}$$

so that equation (A8) can be rewritten as

$$J(k) \cong \mathbf{e}^{\mathrm{T}}(k-1)[\mathbf{I} - \alpha(\mathbf{S}^{\mathrm{T}}(k)\hat{\mathbf{S}}(k) + \hat{\mathbf{S}}^{\mathrm{T}}(k)\mathbf{S}(k))]\mathbf{e}(k-1). \tag{A10}$$

The factor $\mathbf{e}^{\mathrm{T}}(k-1)\mathbf{e}(k-1)$ in this last equation being the cost function at step $(k-1)$ of the adaptive procedure, the link between the cost functions at steps $(k-1)$ and (k) can be written as

$$J(k) \cong J(k-1) - \alpha\mathbf{e}^{\mathrm{T}}(k-1)\mathbf{M}(k)\mathbf{e}(k-1), \tag{A11}$$

in which matrix $\mathbf{M}(k)$ is defined as $\mathbf{M}(k) = \mathbf{S}^{\mathrm{T}}(k)\hat{\mathbf{S}}(k) + \hat{\mathbf{S}}^{\mathrm{T}}(k)\mathbf{S}(k)$. It is interesting to note that matrix $\mathbf{M}$ is symmetric, since from its definition it is clear that $\mathbf{M}^{\mathrm{T}} = \mathbf{M}$. Matrix $\mathbf{M}$ therefore has real eigenvalues. Equation (A11) shows that the cost function is reduced between steps $(k-1)$ and (k) provided that matrix $\mathbf{M}(k)$ is positive definite. Matrix $\mathbf{M}(k)$ being dependent of the step of adaptation, this condition must hold after each update of the controller. Physically, a reduction of the cost function means that the controller converges toward a minimum of the error surface, which is not necessary the global minimum since, because of the secondary source non-linear behaviour, the error surface is likely to exhibit several minima. As demonstrated in reference [24], for example, a necessary and sufficient condition for symmetric matrix $\mathbf{M}(k)$ to be positive definite is that all its eigenvalues are positive.